Release of nitrogenous disinfection by-product precursors in algae-laden water under UV radiation

Weiliang Pan, Yunpeng Cao, Rui Deng, Li Gu, Jian Xu and Changlong Ding

ABSTRACT

Nitrogen-containing organic compounds and nitrogenous disinfection by-products (N-DBPs) in drinking water have attracted attention in the field of water treatment. Metabolites released during algae growth contain a variety of organic nitrogen species, which are called N-DBP precursors. The aim of this paper is to elucidate how N-DBP precursors are released under UV radiation, as well as investigate the variations of their chemical properties. The results show that through UV radiation, the physiological metabolism of algal cells was disordered and the properties of their metabolites were changed. The dissolved organic nitrogen (DON) compound concentration increased rapidly from 5.38 at the beginning to 11.11 mg/L after 30 min of radiation, and then increased steadily from 11.11 to 23.71 mg/L during a further 210 min of radiation. Derivation results of the curves for algae and DON concentration variations shows that when 1×10^{10} algal cells were destroyed, 8.31 mg DON was released into the solution during the first 30 min of radiation. Low dose UV radiation brought a slight decline of the specific N-DBP formation potential due to changes in the extracellular organic matter (EOM) structure without destroying the algal cells, which was conducive to controlling the formation potential of N-DBPs. Long-time UV radiation can bring a significant increase in N-DBP formation potential. After 4 hours of ultraviolet radiation, the total formation potential of N-DBPs in the solution increased from about 84.9 μg/L to about 213.5 μg/L, 2.5 times higher than the initial solution. The N-DBP formation potential increases obviously during the first 10–30 min UV radiation, and then decreases slightly in the subsequent 30–240 min radiation.

Key words | algae-laden water, concentration, metabolites, nitrogenous disinfection by-product (N-DBP) formation potential, release, UV radiation

Weiliang Pan (corresponding author)
Yunpeng Cao
Rui Deng
National Inland Waterway Regulation Engineering Technology Research Center,
Chongqing Jiaotong University,
66 Xuefu Avenue, Chongqing, 400074,
China
E-mail: *pan0316@126.com*

Li Gu
Key Laboratory of the Three Gorges Reservoir Region's Eco-environments,
Ministry of Education,
College of Environment and Ecology,
Chongqing University,
174 Shapingba Road, Chongqing 400045,
China

Jian Xu
Wuhan Municipal Engineering Design & Research Institute Co., Ltd,
40 Changqing Road, Wuhan 40023,
China

Changlong Ding
China Architecture Shanghai Design & Research Institute Co., Ltd,
No. 245 Yunling East Road, Putuo District,
Shanghai,
China

HIGHLIGHTS

- After ultraviolet radiation, the physiological metabolism of algal cells is disturbed and the metabolic properties are changed.
- The concentration of will increase rapidly after 30 min of irradiation, and then steadily during a further 210 min of irradiation.
- Under UV irradiation, the total formation potential of N-DBPs in the solution first increases then decreases with time.

doi: 10.2166/ws.2020.334

INTRODUCTION

In recent decades, urbanisation has accelerated in China. The environmental pollution caused by increasing wastewater discharge is now becoming a serious issue. Rivers and lakes that receive pollutants are now increasingly suffering eutrophication problems. Algal blooms can frequently be found across the country, causing unpleasant environmental conditions and urban water supply crises (Qin *et al.* 2010). China is now in a stage of rapid economic development, and the resulting pollution, as well as water eutrophication, is expected to persist for a long time. It has been reported that cyanobacterial blooms lead to rapid deterioration of water quality (Schaeffer *et al.* 2018). In treatment of algae-containing water, larger dosages of coagulants are needed, and it is difficult to prevent toxin release, especially in the disinfection process (Jiang *et al.* 1993).

Based on the above analysis, it is necessary to eliminate algae from source water. A variety of techniques have been investigated and applied, such as coagulation, flotation, filtration, ozonation, chlorination, oxidation by potassium permanganate, and electrochemical and ultrasonic treatments. Previous studies have shown that ultraviolet (UV) radiation, especially shortwave ultraviolet radiation (UV-C at 254 nm), is highly effective for the removal of algae (Barrado-Moreno *et al.* 2017). UV radiation destroys the cell structure of algae, and thus the integrity of the cells and the substances inside the cells were changed. In addition, compared with other chemical agents, UV radiation is much more efficient in algae destruction, with no chemical waste and fewer by-products (Bischof *et al.* 2000; Wan *et al.* 2019).

Although UV radiation can effectively remove algae, it cannot solve the problems caused by the release of algal organic matter (AOM), which may threaten human health. AOM has been described in most algal species, such as *Microcystis aeruginosa*, *Scenedesmus quadricauda*, *Anabaena flos-aquae*, *Fragilaria crotonensis*, and *Chlamydomonas geitleri* (Tang *et al.* 2017). In the chlorination treatment of wastewater containing algae, when UV radiation is introduced, the removal of *M. aeruginosa* cells can be enhanced, and the chlorination reaction of algae cells can be enhanced by UV light, and the formation of DBPs can also be reduced (Chen *et al.* 2020). Under UV radiation, the physiological metabolism of algal cells is disordered and the metabolites are abnormal; thus, AOM is released from the algal cells (Wang *et al.* 2015). AOM is generally classified into two fractions: intracellular organic matter (IOM) and extracellular organic matter (EOM). IOM is commonly derived from the cleavage of algal cells, whereas EOM originates from the metabolic activity of the algae. AOM typically includes oligosaccharides, polysaccharides, proteins, peptides, amino acids, aromatic compounds, and small amounts of organic acids (Henderson *et al.* 2008; Li *et al.* 2012). The proteins, peptides, and acids are typical dissolved organic nitrogen compounds (DONs). These nitrogenous substances have been reported as the main precursors of nitrogenous disinfection by-products (N-DBPs), which are transformed into DBPs further in the process of disinfection (Chang *et al.* 2013).

Therefore, it is necessary to carry out in-depth investigation of N-DBP precursor release under UV radiation, with the aims of controlling the yields of N-DBPs and ensuring drinking water safety. As acknowledged, there has been little study of algal cell abnormality and release of metabolites and DONs during UV treatment (Wert *et al.* 2013). In particular, the variation of the N-DBP formation potential of algae-laden water under UV treatment is still unknown. Therefore, this study aims to elucidate the variations of the concentrations and structures of N-DBP precursors released during UV radiation. The variation of DON formation and the corresponding N-DBP formation potential associated with UV treatment are of particular concern. This study has great guiding significance with respect to the generation and control of N-DBPs under UV radiation.

METHODS

Algae cultivation procedure

M. aeruginosa (blue-green algae, Collection No. FACHB-905) was purchased from the Institute of Hydrobiology of the Chinese Academy of Sciences (Wuhan, China). *M. aeruginosa* cells in the exponential phase were inoculated in

700 ml BG11 medium, contained in 1,000 mL flasks. The algal cells were maintained in an incubator at 298 K, with illumination at 2,000 lx under a 12 h light/12 h dark (12 L/12D) regimen. There was no medium supplement during the culture process. The algae in stationary growth phases were isolated and concentrated. In the UV radiation process, the concentrated algae solution was diluted to a working solution of about 1×10^{10} cfu/L.

Reagents

All chemicals were of analytical grade or higher purity. Potassium persulfate ($K_2S_2O_8$) came from United Initiators (Shanghai) Co., Ltd. Trichloroacetonitrile (TCAN), Dichloroacetonitrile (DCAN), and Dibromoacetonitrile (DBAN) standard products were purchased from Shanghai Anpu Scientific Instrument Co., Ltd. Methyl tert-butyl ether and 1,2-Dibromopropane were from Sigma-Aldrich, China. N, N-Diethyl-p-phenylenediamine (DPD) and sodium hypochlorite solution, potassium permanganate ($KMnO_4$), potassium dihydrogen phosphate (KH_2PO_4) and other agents came from Chengdu Kelon Chemical Reagent Factory.

Experimental procedure

In this study, UV lamps were used to simulate UV radiation treatment of algae-laden water. Three specially modified quartz glass UV lamps were waterproofed at both ends for the immersion UV-C irradiation system. Each UV lamp had a power of 6 watts and a wavelength of 253.7 nm. The radiation intensity of the immersion UV radiation system was about 2,500 mJ/cm^2. Samples were taken at certain intervals and excessive Na_2SO_3 was immediately used to treat it. The water sample was adjusted to pH 7.0 by a certain concentration of hydrochloric acid and sodium hydroxide, and a buffer solution of 0.5M phosphate was added to it. At the same time, 50 mL samples were collected after the reaction for the analysis of disinfection by-products.

Analytical methods

Total organic carbon (TOC) in solution includes particulate organic carbon (POC) and dissolved organic carbon (DOC). In this research, DOC was the focus, and was measured by a TOC analyser (Liqui TOC II, Elementar, Germany). DON in the water samples was measured by subtracting inorganic nitrogen from total nitrogen. The concentration of algal cells was determined using a blood counting plate. Each counting plate was divided into two identical counting zones by H-shaped grooves. It has been reported that optical density at 680 nm (OD680) can reflect the concentration of algal cells in algal suspension to a certain extent, and is also used to reflect algae concentration. A UV254 test is typically associated with unsaturated functional groups and aromatic organic matter, and can reflect the amounts of these substances in solution (Leloup *et al.* 2013). Measurement of OD680 and UV254 was carried out using a UV–visible spectrophotometer (DR5000, HACH, America) coupled with a quartz cuvette, with an optical path of 1 cm. Specific ultraviolet absorbance (SUVA) has been reported to have a positive correlation with the aromaticity of a substance and the amount of hydrophobic material, and its calculation formula is SUVA = UV254 × 100/TOC (L/mg·m).

Three-dimensional (3D) excitation–emission matrix (EEM) fluorescence spectroscopy (F-7000 FL Spectrophotometer, Hitachi, Japan) was used to characterise AOM during reaction. In this paper, the excitation (Ex) wavelength was set from 200 to 550 nm at 5 nm scanning intervals, and the emission (Em) wavelength was set from 220 to 650 nm with the same sampling intervals. The excitation and emission slits were set at 5 nm, with a scanning speed of about 60,000 nm/min (Mao *et al.* 2020).

Determination of N-DBP formation potential

The solution was sampled and filtered after different irradiation times. Filtrates without algal cells were chlorinated to determine their N-DBP potential. The chlorination was conducted under a temperature of 293 K with excess chlorine dosage (available chlorine/TOC $\geq$5/1). The reaction was conducted under dark conditions. After seven days of reaction, reductant was added to terminate the chlorination reaction.

N-DBPs studied in this paper included DCAN (dichloroacetonitrile), TCAN (trichloroacetonitrile), TCNM (trichloronitromethane), and 1,1,1-TCP (1,1,1-trichloro-2-propanone). Gas chromatography (GC-2010Plus, Shimadzu,

Japan) coupled with an electron capture detector (ECD) and an HP5 column (30 m × 0.25 mm, ID × 0.25 μm) was used to measure these N-DBPs (Chu *et al.* 2015; Chen *et al.* 2020). The carrier gas was high-purity nitrogen (99.99%) at a flow rate of 1.0 mL/min. The temperatures of the injector and the ECD detector were 473 and 563 K, respectively. The temperature of the oven was programmed to begin at 308 K for 9 min, ramp to 313 K at 2 K/min and hold for 1 min, ramp to 353 K at 20 K/min, and then ramp to 433 K at 40 K/min and hold for 4 min (Xie *et al.* 2013).

RESULTS AND DISCUSSION

Variations of algal cells, OD680, and UV254 under UV radiation

Figure 1 shows variations of algae concentration, OD680, and UV254 during UV radiation. The algae concentration decreased rapidly from 0.94×10^{10} to 0.34×10^{10} cfu/L during the first 30 min of radiation. With further UV radiation, the algae concentration decreased incrementally. After 240 min of radiation, the algae concentration was about 0.28×10^{10} cfu/L, showing that about 70% of algal cells were damaged. OD680 tests are commonly used to reflect the concentration of algal cells in algal suspension; thus, its concentration variation shows a close curve with that of the algae concentration. It decreased from 0.51 to 0.17 cm^{-1}. The death of algal cells in a short time caused significant change in the colour of the solution from green to khaki brown. Microscopic examination (shown in Figure 2) revealed that some cellular boundaries were blurred after radiation, indicating that the cells had been damaged and inclusions released (Tao *et al.* 2010, 2013). In contrast with the decreases in algae concentration and OD680, UV254 presented an increasing trend. In the initial stage, UV254 decreased rapidly from 0.62 to 0.58 cm^{-1} after 10 min of radiation. This may have been caused by the partial oxidation of EOM in solution. Further radiation would cause a large number of algal cell deaths, and the rapid increase of UV254 at 10–30 min of reaction confirmed that large amounts of cell inclusions were released from inside the cells to the solution. UV254 reached its peak value after 60 min of radiation, and showed a slight decrease during subsequent radiation, which can be ascribed to the oxidation of inclusions. UV254 is regarded as associated with unsaturated functional groups and aromatic organic matter. Thus, the increase of UV254 indicates that much greater amounts of dissolved aromatic organic substances appeared during the reaction. These dissolved aromatic organic substances were aromatic organic proteins, which can be classified as organic nitrogen compounds (DONs). They were reported as the main source of N-DBP precursors that would be transformed into DBPs during chlorination.

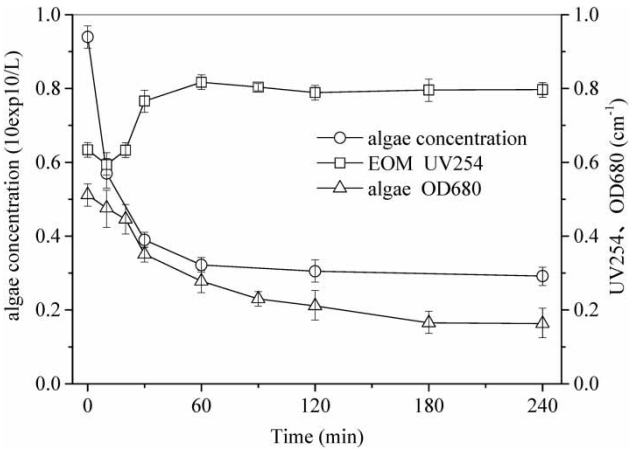

Figure 1 | Variations of algae concentration, OD680, and UV254 under UV radiation.

Variations of different nitrogen species during radiation

Figure 3 shows the concentration variations of different nitrogen species during UV radiation. The concentration of dissolved total nitrogen (DTN) increased, whereas those of NO_3^- and NH_4^+-N decreased. The concentration of NO_2^- was so low that its variation could hardly be identified. The concentration of DON can be calculated by subtracting inorganic nitrogen from DTN. Thus, a significant increase was observed in the DON concentration. The figure also shows that the DON concentration rose rapidly from 5.4 to 11.1 mg/L during the first 30 min of radiation. Subsequently, the concentration rose steadily from 11.1 to 23.7 mg/L. However, the increase rate of the DON concentration was reduced. The increase of the DTN concentration was attributed to the release of inclusions caused by the UV radiation. In addition, the results indicate that the rate of

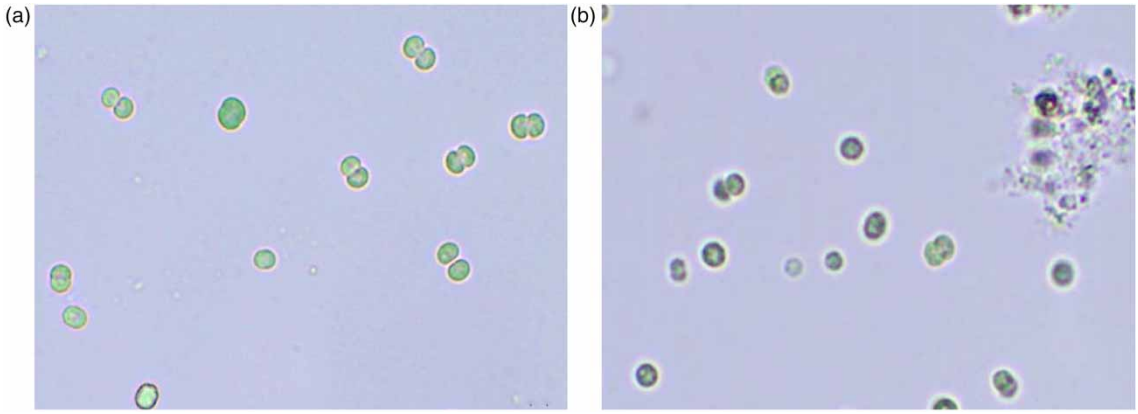

Figure 2 | *Microcystis aeruginosa* before and after UV radiation stress. (a) before ultraviolet radiation, (b) after ultraviolet radiation.

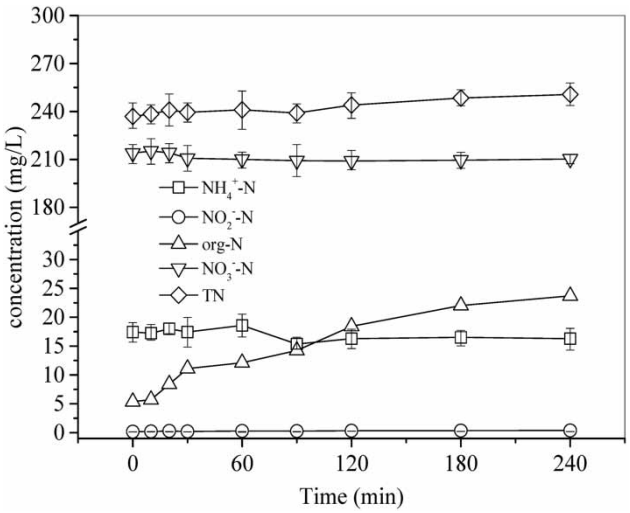

Figure 3 | EOM nitrogen concentration under UV radiation.

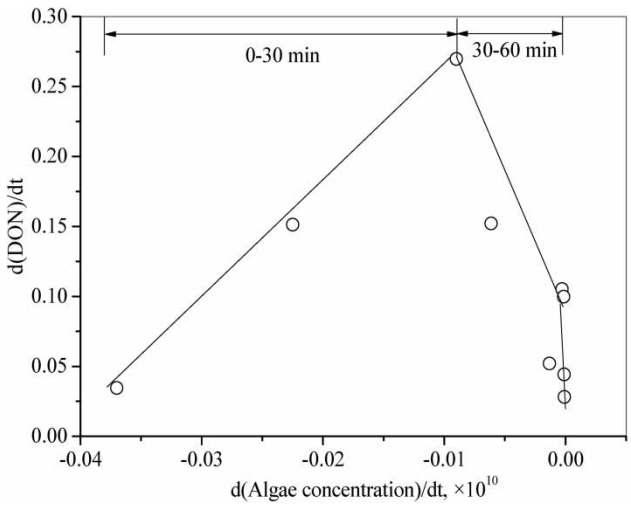

Figure 4 | Relationship between DON increase and decrease in algae cells.

algal cell destruction in the initial stage was much faster than that found in the middle and final stages of radiation.

Figures 1 and 3 indicate that, with the destruction of the algal cells, the DON concentration increased correspondingly. Therefore, it is necessary to determine the relationship between the increase of DON concentration and the decrease of algal cells. For this purpose, first, the curves for algae and DON concentration variations were derived. The algae concentration was set as the X-axis, and the DON concentration was set as the Y-axis. The relationship between DON increase and algae cell decrease is shown in Figure 4. This figure shows that there was a linear relationship between d(algae concentration)/dt and d(DON)/dt. It is widely acknowledged that the derivation result of the variation curve of the algae and DON concentrations reflect the concentration variation over a short time. Therefore, the figure shows that during the first 0–30 min of radiation, the destruction of algal cells led directly to the increase of the DON concentration. The rate of algae destruction was reduced during further radiation, and their relationship was reversed. The linear fit result for this relationship during the first 30 min of radiation was about 8.3 mg DON/10^{10} cfu/L, showing that when 1×10^{10} algal cells were destroyed, 8.3 mg of DON would be released into the solution. In the mid and late stages of the radiation process, because of the reduced algae concentration in the solution, the rates of algae destruction

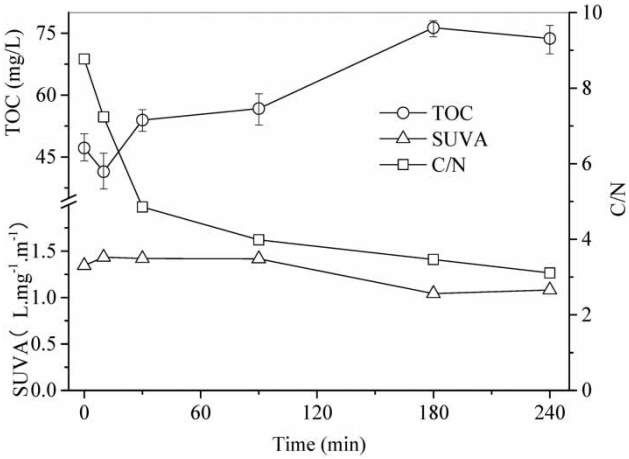

Figure 5 | Variation of TOC concentration, C/N and SUVA under UV radiation.

and the generation of dissolved nitrogenous substances were reduced.

Variations of TOC, C/N, and SUVA

Figure 5 shows the variations of the DOC concentration, carbon-to-nitrogen ratio (C/N), and SUVA during UV radiation. Under UV radiation, the DOC concentration increased rapidly after initial short-term adaptation. The short-term adaptation during the first 5–10 min may have been caused by the degradation and transformation of EOM in solution. Subsequently, the DOC in solution underwent a gradual increase from 47.6 to 76.3 mg/L. The C/N ratio reflects the percentage of nitrogenous substances in the solution; a lower value of C/N indicates that a greater proportion of nitrogenous fractions can be found in the solution, which may present higher N-DBP potential during disinfection. The value of C/N declined rapidly from an initial value of 8.8–4.9 after 30 min of radiation. Subsequently, this decline slowed down, and the final C/N value at the end of the reaction was about 3.1. The low C/N value of the solution means that large quantities of nitrogenous substances were released into the solution, and the solution may present higher N-DBP potential during disinfection. SUVA is used to measure the aromaticity of substances in water. A high SUVA value indicates that humic acid, fulvic acid, macromolecular organic compounds, unsaturated double bonds, and aromatic organic compounds comprise a high proportion on the constituents of dissolved substances. Compared with the variations of TOC and C/N, the values of SUVA were relatively stable in the early stages of the reaction.

Three-dimensional EEM spectra for different samples

Three-dimensional EEM spectra can be used to classify organic pollutants and provide information on their contents (Sheng & Yu 2006). The fluorescence properties of DOM differ in various natural sources. Based on the locations of the fluorescence peaks of various types of DOM in natural environments, the results can be divided into five regions: regions I and II (Ex < 250 nm, Em < 380 nm) indicate the presence of aromatic proteins, region III (Ex < 250 nm, Em > 380 nm) indicates the presence of fulvic acid, region IV (Ex > 250 nm, Em < 380 nm) indicates the presence of dissolved microbial metabolites, and region V (Ex > 250 nm, Em > 380 nm) indicates the presence of humic acid (Guo *et al.* 2014). Regions I, II, and IV can be used to represent organic nitrogenous species. Regions III and V represent organic carbon compounds.

Figure 6 shows the 3D-EEM spectra for different samples under UV radiation. The position and intensity of each EEM peak are shown in Table 1. There were three peaks in the spectra. Peak A was located in region V, peak B was located in region IV, and peak C was located in region III. The intensity of peak A decreased as the reaction proceeded, accompanied by a slight blue shift (the values of lambda Ex and lambda Em became smaller). This finding indicates that the contents of electron-donating groups on the aromatic rings of humic acid and fulvic acid in the EOM were higher. Peak B decreased significantly with increasing UV radiation time, and the intensity of the peak was only 6.6% of the initial value after 3 hours of radiation. In addition, a blue shift was observed. Thus, UV radiation can significantly depress the stability of the cell metabolites, resulting in decomposition of the organic matter. The absorption peaks in regions III and V nearly disappeared after 240 min of radiation.

N-DBP formation potential of EOM under UV radiation

The N-DBPs mentioned in this paper include DCAN, TCAN, TCNM, and 1,1,1-TCP. These substances are all

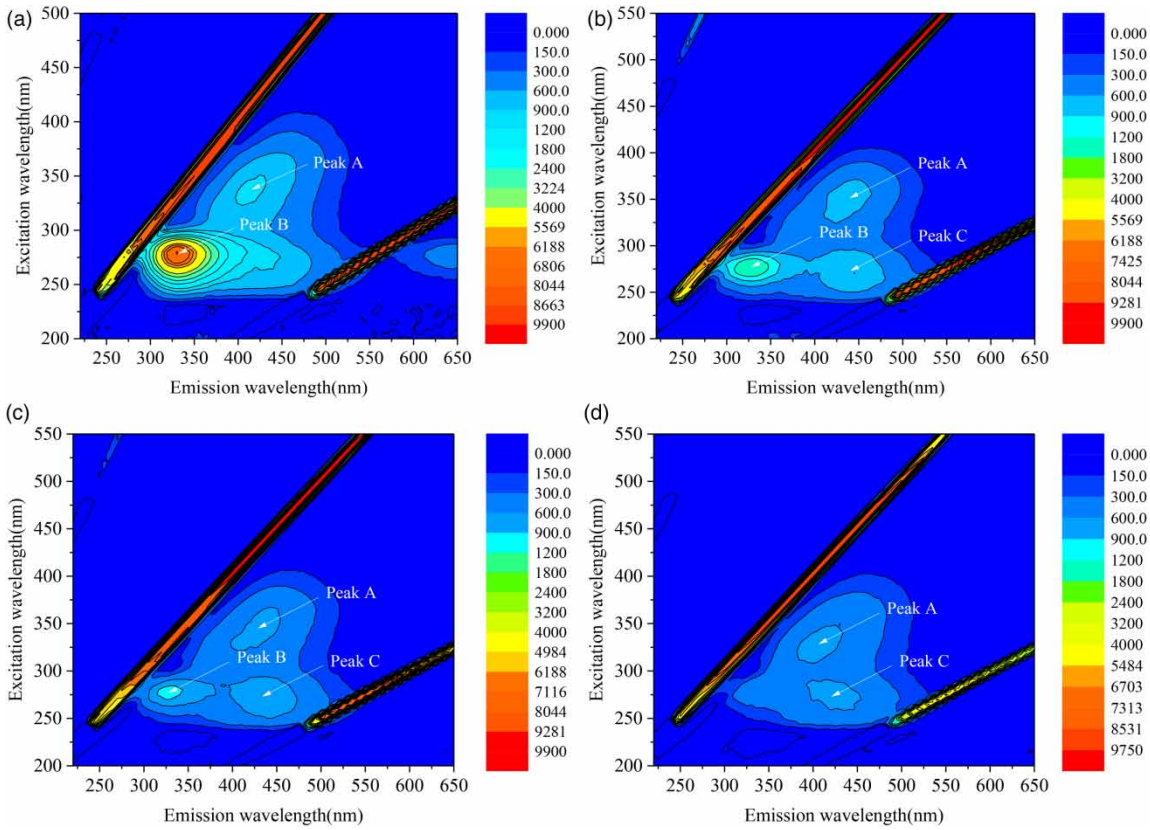

Figure 6 | 3D-EEM spectra for different samples obtained in UV radiation (a. 0 min, b. 60 min, c. 120 min, d. 240 min).

Table 1 | The position and intensity of each EEM peak

	Region V (Peak A)		Region IV (Peak B)		Region III (Peak C)	
Sample[a]	Ex/Em[b]	Int.[c]	Ex/Em[b]	Int.[c]	Ex/Em[b]	Int.[c]
0 min (a)	340/415	825.4	275/330	8043		
60 min (b)	355/440	759.3	275/325	1573	270/445	902.9
120 min (c)	345/430	660.7	275/325	1009	270/440	800.4
180 min	340/415	696.7	280/330	968.1	275/430	813.9
240 min (d)	325/405	685.8	280/345	535.2	275/430	667.3

[a]Samples (a), (b), (c) and (d) refer to the four spectra shown in Figure 6.
[b]Ex/Em: Excitation wavelength/Emission wavelength (nm).
[c]Int.: Radiation intensity.

typical N-DBPs (Chu *et al.* 2015). Figure 7 shows the formation potential of these N-DBPs for dissolved AOM obtained under UV radiation. The figure shows that the formation potential of the initial solution was about 84.9 μg/L. After 6 hours of UV radiation, the total N-DBP formation potential was about 213.5 μg/L, 2.5 times higher

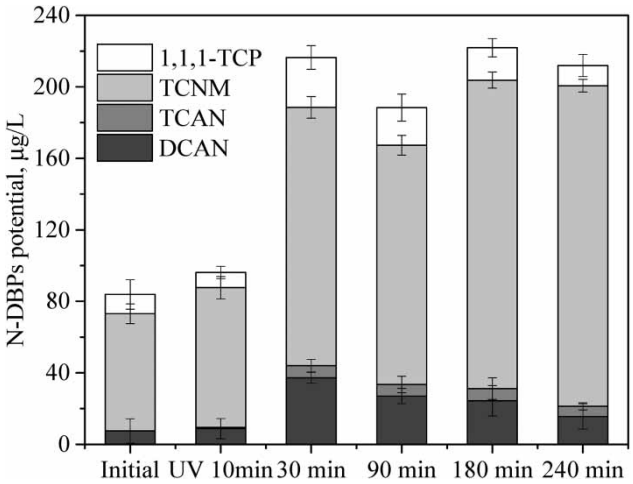

Figure 7 | N-DBPs potential for EOM obtained in UV radiation.

than that of the initial solution. In addition, the formation potential increased significantly from 84.9 to 218.7 μg/L under the initial 10–30 min of UV radiation. Further radiation for 30–240 min could hardly cause any prominent changes in formation potential, which varied from 192.3 to 218.7 μg/L. Among the identified N-DBPs induced by UV irradiation, TCNM dominated, accounting for 83.9% of the total amount of N-DBPs after 6 hours of radiation. The proportions of DCAN and 1,1,1-TCP were the next largest, at about 7.7% and 5.3% of the total amount, respectively. TCAN could hardly be detected in the initial stage, and its concentration increased gradually under UV radiation. After 30 min of radiation, the amount of TCAN formation was about 6.8 μg/L, about 3.1% of the total N-DBP formation potential. After 240 min of radiation, TCAN production accounted for 2.6% of the total. In summary, the N-DBP formation potential increased notably during the first 30 min of UV radiation and then decreased slightly in the subsequent 30–240 min of radiation.

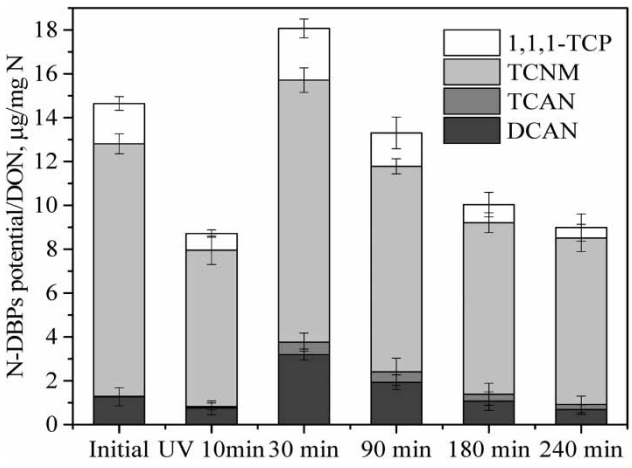

Figure 8 | The amount of N-DBPs potential produced by per milligram of DON.

To further elucidate the N-DBP formation potential variation, the amount of N-DBPs potentially produced per milligram of DON (specific N-DBP formation potential) was calculated, and the results are shown in Figure 8. Initially, the specific N-DBP formation potential was about 14.7 μg/mgN. After 10 min of UV radiation, it declined to about 8.7 μg/mgN. This reduction can be ascribed to the oxidation of the EOM in the solution, which changed the EOM structure and decreased its tendency to conversion to N-DBP. The specific formation potential increased significantly to about 18.1 μg/mgN after 30 min of radiation, which is about 2.1 times that obtained after 10 min of treatment. Figure 3 indicates that after 30 min radiation, the DON concentration increased dramatically. The remarkable increase in the specific formation potential behind the background of DON release, the concentration of which is the denominator to calculate the specific formation potential, confirms that the nitrogenous substances in the inclusions of the algal cells were the main precursors of N-DBP formation. A further 30–240 min of UV radiation led to a consistent decline in the specific N-DBP formation potential. At the end of the reaction (240 min of radiation), the specific N-DBP formation potential was about 9.1 μg/mgN, about half of the potential obtained after 30 min of radiation, indicating that the destruction or oxidation of the dissolved substances induced by UV radiation was conducive to controlling N-DBP precursors.

CONCLUSION

From the results shown above, the following conclusions can be drawn. UV radiation can rapidly destroy algal cells and cause the release of cell inclusions. DON concentration in the solution rose rapidly during the first 30 min of radiation, and climbed at a slower rate during subsequent radiation. The fitting results indicate that when 1×10^{10} algal cells were destroyed under radiation, 8.3 mg of DON would be released during the initial stage of radiation. The

3D-EEM analysis showed that there were higher contents of electron-donating groups on the aromatic rings of humic acid and fulvic acid in the EOM after radiation.

The N-DBP formation potential of the raw solution was about 84.9 μg/L, with a specific formation potential of 14.7 μg/mgN. UV radiation was confirmed to cause significant improvement to this potential. It increased rapidly to about 213.5 μg/L during the first 10–30 min of radiation and then changed little during further radiation. However, the specific formation potential changed via different paths. It declined during the first 10 min of radiation to about 8.7 μg/mgN because of the oxidation of the EOM in solution. Then, 10–30 min of radiation led to a significant increase to 18.1 μg/mgN because of the release of cell inclusions. Further radiation caused partial oxidation of the dissolved substances; consequently, a consistent decline of the specific N-DBP formation potential was observed. Therefore, in treating algae-laden water, the radiation time should be controlled at less than 10 min.

ACKNOWLEDGEMENT

The authors would like to acknowledge the financial support for this work provided by the Ministry of Housing and Urban-Rural Development Science and Technology Project (2016-K6-025) and Chongqing Science and Technology Bureau Project (cstc2017shmsA20011).

DATA AVAILABILITY STATEMENT

All relevant data are included in the paper or its Supplementary Information.

REFERENCES

Barrado-Moreno, M. M., Beltran-Heredia, J. & Martin-Gallardo, J. 2017 Degradation of microalgae from freshwater by UV radiation. *J. Ind. Eng. Chem.* **48**, 1–4.

Bischof, K., Hanelt, D. & Wiencke, C. 2000 Effects of ultraviolet radiation on photosynthesis and related enzyme reactions of marine macroalgae. *Planta* **211**, 555–562.

Chang, H., Chen, C. & Wang, G. 2013 Characteristics of C-, N-DBPs formation from nitrgen-enriched dissolved organic matter in raw water and treated wastewater effluent. *Water Res.* **47**, 2729–2741.

Chen, Y., Bai, F., Li, Z., Xie, P., Wang, Z., Feng, X., Liu, Z. & Huang, L.-Z. 2020 UV-assisted chlorination of algae-laden water: cell lysis and disinfection byproducts formation. *Chem. Eng. J.* **383**, 123165.

Chu, W. H., Li, D. M., Gao, N. Y., Templeton, M. R., Tan, C. Q. & Gao, Y. Q. 2015 The control of emerging haloacetamide DBP precursors with UV/persulfate treatment. *Water Res.* **72**, 340–348.

Guo, L., Lu, M. M., Li, Q. Q., Zhang, J. W., Zong, Y. & She, Z. L. 2014 Three-dimensional fluorescence excitation-emission matrix (EEM) spectroscopy with regional integration analysis for assessing waste sludge hydrolysis treated with multi-enzyme and thermophilic bacteria. *Bioresource Technol.* **171**, 22–28.

Henderson, R. K., Baker, A., Parsons, S. A. & Jefferson, B. 2008 Characterisation of algogenic organic matter extracted from cyanobacteria, green algae and diatoms. *Water Res.* **42**, 3435–3445.

Jiang, J. Q., Graham, N. J. D. & Harward, C. 1993 Comparison of polyferric sulfate with other coagulants for the removal of algae and algae-derived organic-matter. *Water Sci. Technol.* **27** (11), 221–230.

Leloup, M., Nicolau, R., Pallier, V., Yepremian, C. & Feuillade-Cathalifaud, G. 2013 Organic matter produced by algae and cyanobacteria: quantitative and qualitative characterization. *J. Environ. Sci.* **25**, 1089–1097.

Li, L., Gao, N. Y., Deng, Y., Yao, J. J. & Zhang, K. J. 2012 Characterization of intracellular & extracellular algae organic matters (AOM) of microcystic aeruginosa and formation of AOM-associated disinfection byproducts and odor & taste compounds. *Water Res.* **46**, 1233–1240.

Mao, Y. F., Li, H., Liu, X., Fu, H., Liu, Y. & He, Q. 2020 Nanoplastics display strong stability in aqueous environments: insights from aggregation behaviour and theoretical calculations. *Environ. Pollut.* **258**, 113760.

Qin, B. Q., Zhu, G. W., Gao, G., Zhang, Y. L., Li, W., Paerl, H. W. & Carmichael, W. W. 2010 A drinking water crisis in lake taihu, China: linkage to climatic variability and lake management. *Environ. Manage.* **45**, 105–112.

Schaeffer, B. A., Bailey, S. W., Conmy, R. N., Michael, G., Ignatius, A. R., Johnston, J. M., Keith, D. J., Lunetta, R. S., Parmar, R., Stumpf, R. P., Urquhart, E. A., Werdell, P. J. & Wolfe, K. 2018 Mobile device application for monitoring cyanobacteria harmful algal blooms using sentinel-3 satellite ocean and land colour instruments. *Environ. Modell. Software.* **109**, 93–103.

Sheng, G. P. & Yu, H. Q. 2006 Characterization of extracellular polymeric substances of aerobic and anaerobic sludge using three-dimensional excitation and emission matrix fluorescence spectroscopy. *Water Res.* **40**, 1233–1239.

Tang, X. M., Zheng, H. L., Gao, B. Y., Zhao, C. L., Liu, B. Z., Chen, W. & Guo, J. S. 2017 Interactions of specific

extracellular organic matter and polyaluminum chloride and their roles in the algae-polluted water treatment. *J. Hazard. Mater.* **332**, 1–9.

Tao, Y., Zhang, X. H., Au, D. W. T., Mao, X. Z. & Yuan, K. 2010 The effects of sub-lethal UV-C irradiation on growth and cell integrity of cyanobacteria and green algae. *Chemosphere* **78**, 541–547.

Tao, Y., Mao, X. Z., Hu, J. Y., Mok, H. O. L., Wang, L. Y., Au, D. W. T., Zhu, J. & Zhang, X. H. 2013 Mechanisms of photosynthetic inactivation on growth suppression of microcystis aeruginosa under UV-C stress. *Chemosphere* **93**, 637–644.

Wan, Y., Xie, P. Y., Wang, Z. P., Ding, J. Q., Wang, J. W., Wang, S. L. & Wiesner, M. R. 2019 Comparative study on the pretreatment of algae-laden water by UV/persulfate, UV/chlorine, and UV/H_2O_2: variation of characteristics and alleviation of ultrafiltration membrane fouling. *Water Res.* **158**, 213–226.

Wang, B. L., Wang, X., Hu, Y. W., Chang, M. X., Bi, Y. H. & Hu, Z. Y. 2015 The combined effects of UV-C radiation and H_2O_2 on microcystis aeruginosa, a bloom-forming cyanobacterium. *Chemosphere* **141**, 34–43.

Wert, E. C., Dong, M. M. & Rosario-Ortiz, F. L. 2013 Using digital flow cytometry to assess the degradation of three cyanobacteria species after oxidation processes. *Water Res.* **47**, 3752–3761.

Xie, P. C., Ma, J., Fang, J. Y., Guan, Y. H., Yue, S. Y., Li, X. C. & Chen, L. W. 2013 Comparison of permanganate preoxidation and preozonation on algae containing water: cell integrity, characteristics, and chlorinated disinfection byproduct formation. *Environ. Sci. Technol.* **47**, 14051–14061.

First received 9 March 2020; accepted in revised form 13 November 2020. Available online 27 November 2020